

Rare-earth oxides promoted Pd electrocatalyst for formic acid oxidation

Lusheng Xiao,^{†a} Danqi Jia,^{†a} Chen Chen,^a Tingting Liu,^{*a} Xiaofeng Zhang,^a Qiu Feng Huang,^{*a} Mohd Ubaidullah,^b Yuzhi Sun,^c Shengyun Huang,^{*c} and Zonghua Pu^{*a}

a. Fujian Provincial Key Laboratory of Advanced Materials Oriented Chemical Engineering, College of Chemistry & Materials Science, Fujian Normal University, Fuzhou, Fujian 350007, P. R. China.

b. Department of Chemistry, College of Science, King Saud University, Riyadh 11451, Saudi Arabia.

c. Ganjiang Innovation Academy, Key Laboratory of Rare Earths, Chinese Academy of Sciences, Ganzhou 341000, P. R. China

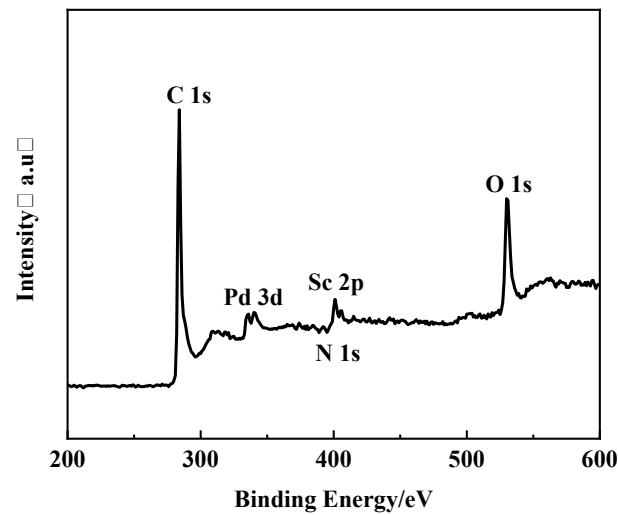


Figure S1. XPS survey spectrum of the Pd- $\text{Sc}_2\text{O}_3/\text{N-rGO-2/3}$.

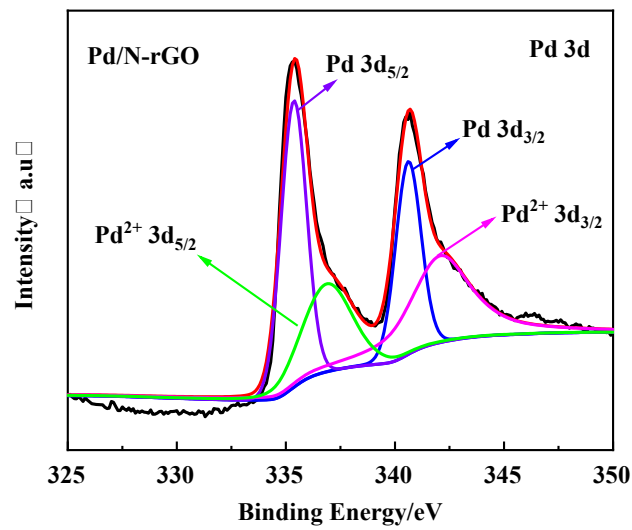


Figure S2. XPS spectrum of Pd 3d for Pd/N-rGO.

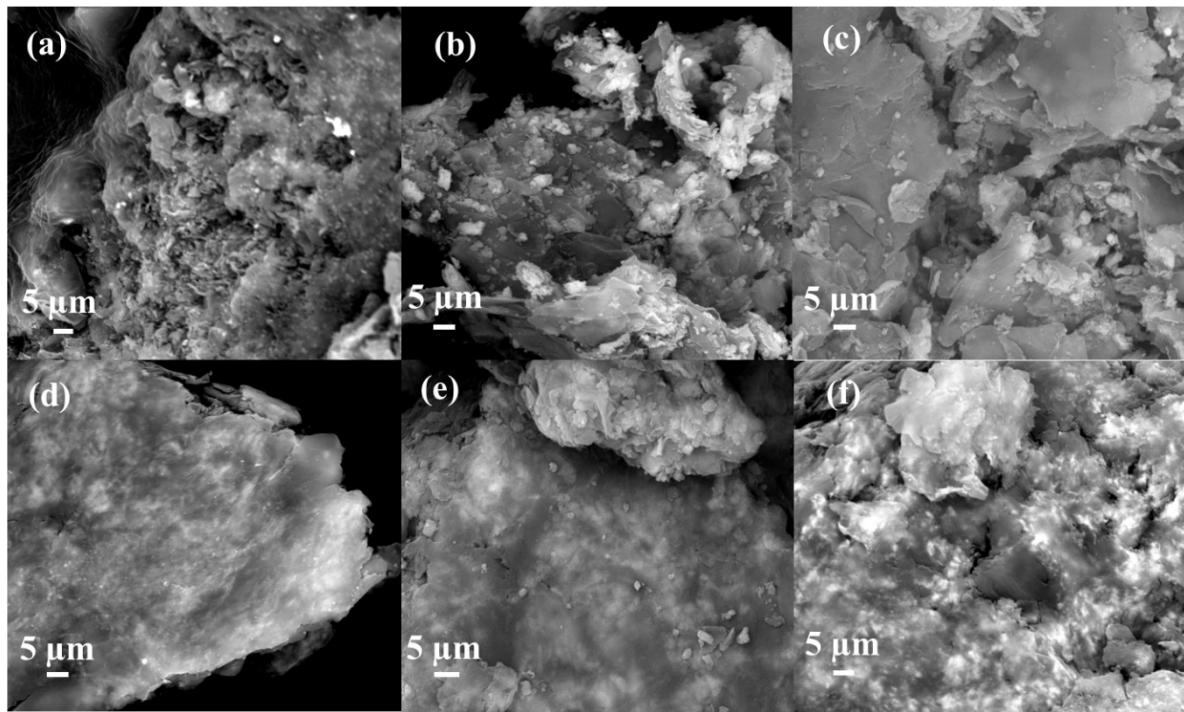


Figure S3. SEM images of (a) Pd/N-rGO and (b-f) Pd-Sc₂O₃/N-rGO-x. SEM images of (b) Pd-Sc₂O₃/N-rGO-1/3, (c) Pd-Sc₂O₃/N-rGO-1/2, (d) Pd-Sc₂O₃/N-rGO-2/3, (e) Pd-Sc₂O₃/N-rGO-1, (f) Pd-Sc₂O₃/N-rGO-3/2.

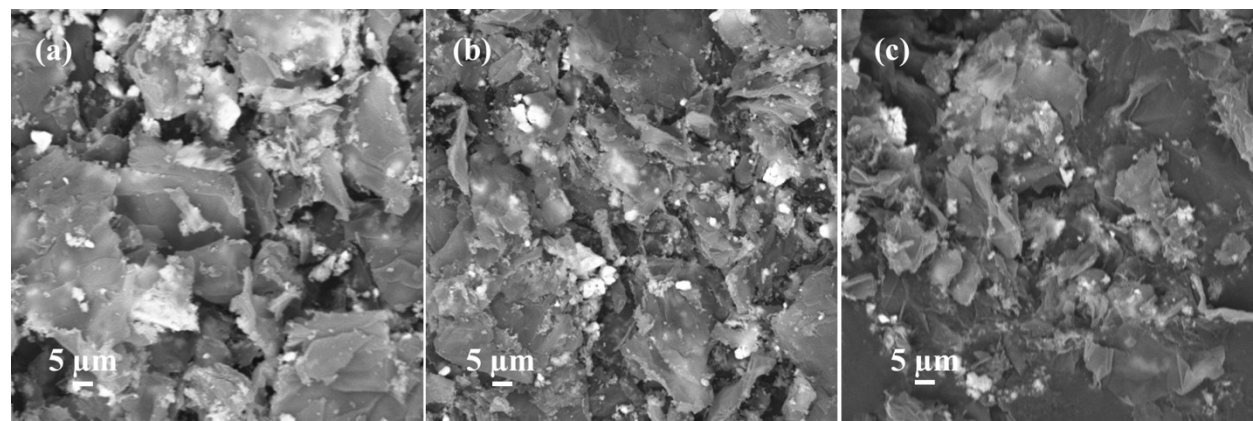


Figure S4. SEM images of (a) Pd-CeO₂/N-rGO, (b) Pd-La₂O₃/N-rGO, (c) Pd-Pr₂O₃/N-rGO.

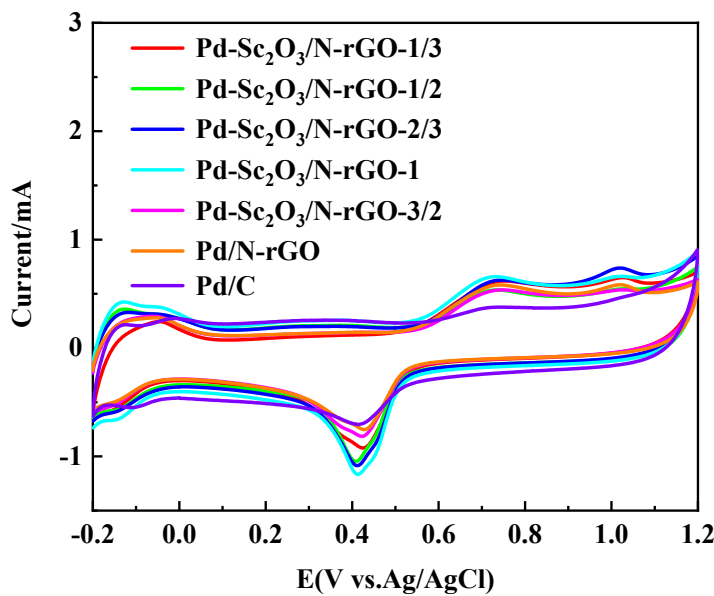


Figure S5. CV curves of Pd/C, Pd/N-rGO and Pd- Sc_2O_3 /N-rGO-x in 0.5 M H_2SO_4 solution.

Supplementary Note 1

The electrochemically surface area (ECSA) is calculated from charges involved in the reduction of Pd oxide processes during the negative scan, according to the equation of $\text{ECSA}_{\text{PdO}} = Q/(C * \text{Pd}_m)$ in the potential range of 0.3-0.6 V, where Q is the integral of the peak from the reduction of Pd oxide, Pd_m is the load of Pd on the electrode, and C is the double-layer capacitance of 0.424 mC cm^{-2} (Ref: *Electrochim. Acta*, 2019, 324, 134816). Based on the CVs, the ECSA_{PdO} of Pd- Sc_2O_3 /N-rGO-2/3 is found to be $5.63 \text{ m}^2 \text{ g}^{-1}$, Pd- Sc_2O_3 /N-rGO-1/3 ($4.59 \text{ m}^2 \text{ g}^{-1}$), Pd- Sc_2O_3 /N-rGO-1/2 ($4.60 \text{ m}^2 \text{ g}^{-1}$), Pd- Sc_2O_3 /N-rGO-1 ($5.61 \text{ m}^2 \text{ g}^{-1}$), Pd- Sc_2O_3 /N-rGO-3/2 ($4.45 \text{ m}^2 \text{ g}^{-1}$), Pd/N-rGO ($4.09 \text{ m}^2 \text{ g}^{-1}$) and Pd/C ($3.52 \text{ m}^2 \text{ g}^{-1}$).

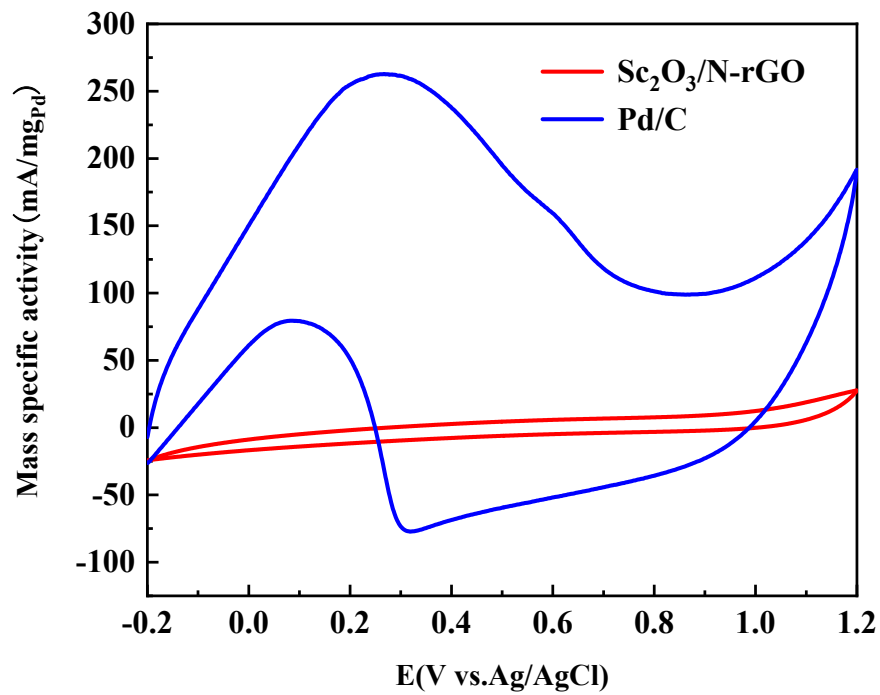


Figure S6 CV curves for $\text{Sc}_2\text{O}_3/\text{N-rGO}$ and Pd/C catalyst in 0.5 M H_2SO_4 + 1.0 M HCOOH solutions.

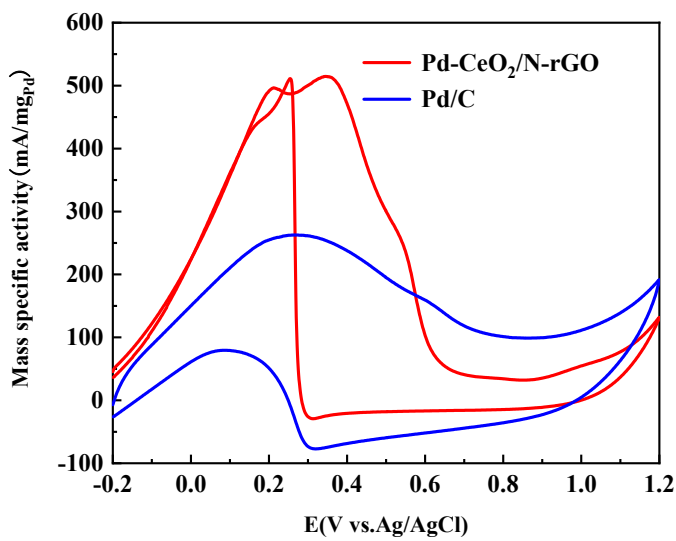


Figure S7 CV curves for Pd-CeO₂/N-rGO and Pd/C catalyst in 0.5 M H₂SO₄ + 1.0 M HCOOH solutions.

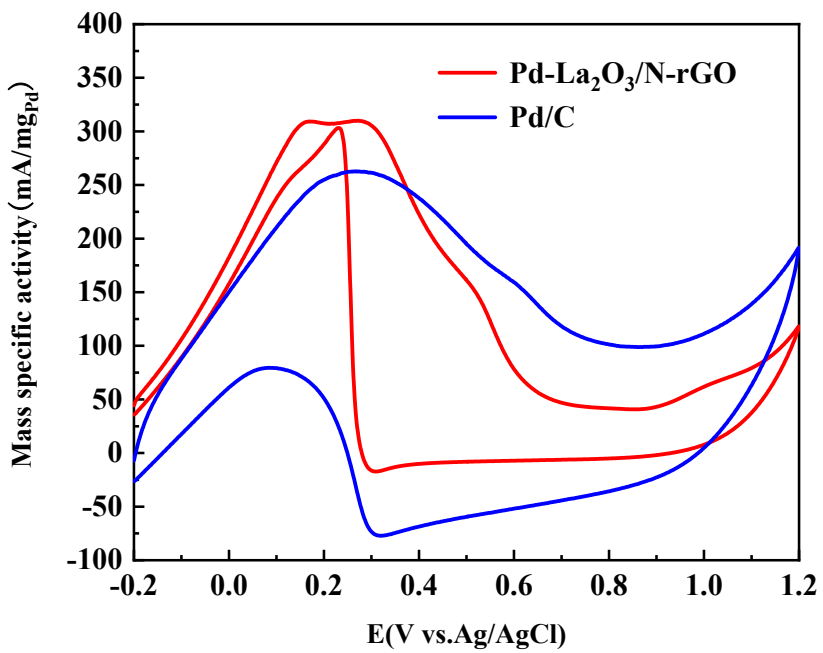


Figure S8 CV curves for Pd-La₂O₃/N-rGO and Pd/C catalyst in 0.5 M H₂SO₄ + 1.0 M HCOOH solutions.

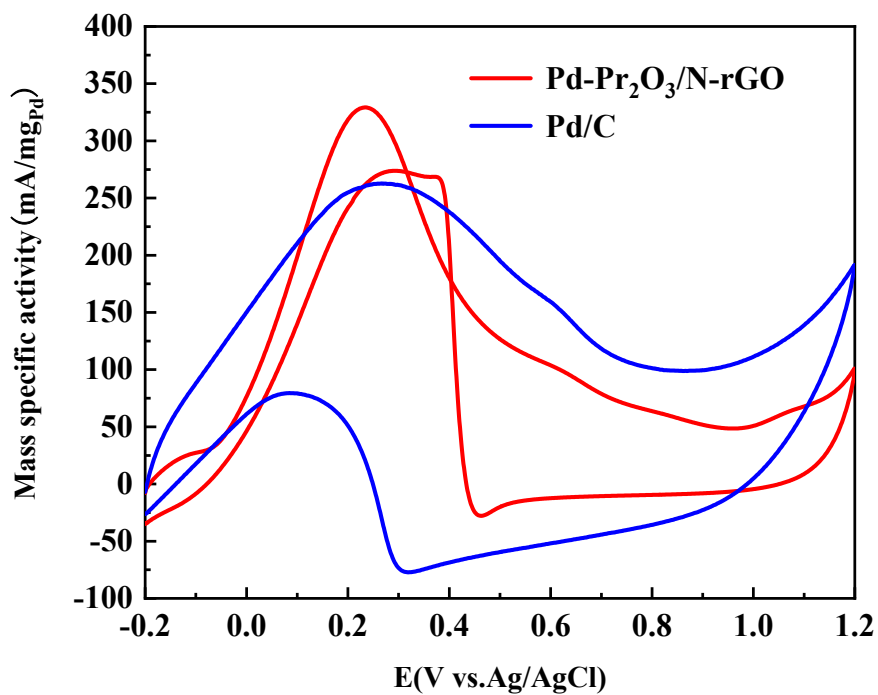


Figure S9 CV curves for Pd-Pr₂O₃/N-rGO and Pd/C catalyst in 0.5 M H₂SO₄ + 1.0 M HCOOH solutions.

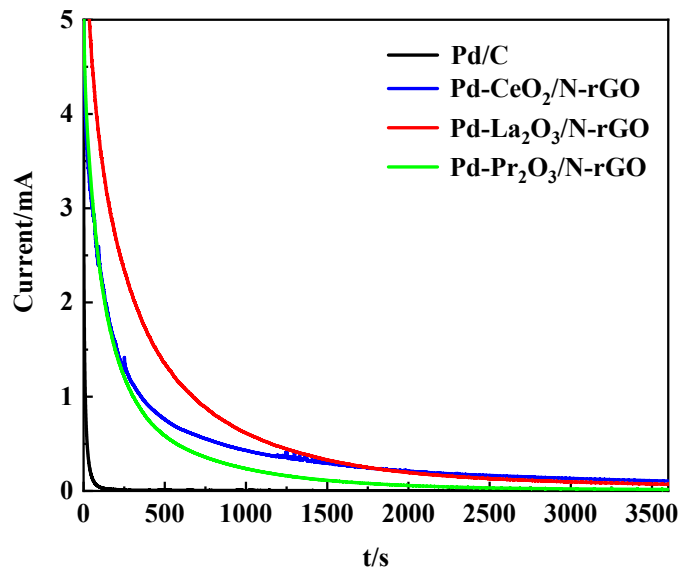


Figure S10 Chronoamperometric curves of Pd-CeO₂/N-rGO, Pd-La₂O₃/N-rGO, Pd-Pr₂O₃/N-rGO and Pd/C in 0.5 M H₂SO₄ + 1 M HCOOH solution.

Table S1. ICP-OES results of Pd-Sc₂O₃/N-rGO-x, Pd/N-rGO, Pd-CeO₂/N-rGO, Pd-La₂O₃/N-rGO and Pd-Pr₂O₃/N-rGO catalysts.

| Samples | Pd (wt.%) |
|--|-----------|
| Pd-Sc ₂ O ₃ /N-rGO-1/3 | 8.89 |
| Pd-Sc ₂ O ₃ /N-rGO-1/2 | 9.35 |
| Pd-Sc ₂ O ₃ /N-rGO-2/3 | 8.27 |
| Pd-Sc ₂ O ₃ /N-rGO-1 | 8.65 |
| Pd-Sc ₂ O ₃ /N-rGO-3/2 | 9.13 |
| Pd/N-rGO | 9.08 |
| Pd-CeO ₂ /N-rGO | 9.47 |
| Pd-La ₂ O ₃ /N-rGO | 8.46 |
| Pd-Pr ₂ O ₃ /N-rGO | 8.30 |

Table S2. Binding energies and their shifts of Pd 3d for Pd/N-rGO and Pd-Sc₂O₃/N-rGO-2/3 catalysts.

| Catalyst | Species | Binding Energy (eV) |
|--|-------------------------|---------------------|
| Pd/N-rGO | Pd(0) 3d _{3/2} | 340.6 |
| | Pd(0) 3d _{5/2} | 335.4 |
| Pd-Sc ₂ O ₃ /N-rGO-2/3 | Pd(0) 3d _{3/2} | 340.3 |
| | Pd(0) 3d _{5/2} | 335.1 |

Table S3. Comparison of electrochemical performance of reported literature and the current work

| Samples | ^a E _f (V) | ^b E _r (V) | ^c J (A/m ²) | ^d J (A/m ²) | ^e I _f /I _b | Ref. |
|--|---------------------------------|---------------------------------|---------------------------------------|---------------------------------------|---|-----------|
| Pd ₃₀ La ₇₀ /rGO | 0.66 | 0.56 | 694.5 | 627 | 1.11 | 1 |
| Pd-CeO ₂ /C | 0.13 | 0.15 | 350 | 300 | 1.16 | 2 |
| Pd ₄ Sm ₆ /rGO | 0.30 | 0.20 | 968 | 589 | 1.6 | 3 |
| PdEuO _x /C | 0.33 | 0.35 | 700 | 650 | 1.06 | 4 |
| Pd ₆ Y ₄ /rGO | 0.36 | 0.46 | 1066 | 1329.5 | 0.80 | 5 |
| Pd/C | 0.28 | 0.12 | 146 | 43 | 3.3 | This work |
| Pd/N-rGO | 0.05 | 0.1 | 162 | 99.5 | 1.62 | This work |
| Pd-Sc ₂ O ₃ /N-rGO-2/3 | 0.36 | 0.43 | 449 | 546 | 0.82 | This work |

^a E_f = forward peak potential.

^b E_r = backward peak potential.

^c J = forward current density.

^d J = backward current density.

^e I_f/I_b = ratio of forward to backward oxidation peak.

References

- [1] H. Ali, F.K. Kanodarwala, I. Majeed, J.A. Stride and M.A. Nadeem, *ACS Appl. Mater. Interfaces*, 2016, **8**, 32581-32590.
- [2] Y. Wang, S. Wang and X. Wang. *Solid-State Lett.*, 2009, **12**, 2009 B73.
- [3] M. Sofian, F. Nasim, H. Ali and M.A. Nadeem, *Int. J. Hydrogen Energy*, 2023, **48**, 16370-16380.
- [4] J. Duan, Q. Li, Y. Fu and J. Chang, *Int J Hydrogen Energy*, 2021, **46**, 39768e77.
- [5] M. Sofian, F. Nasim, H. Ali and M.A. Nadeem, *RSC Adv.*, 2023, **13**, 14306-14316.